

# Charge mobility of perfluoroarene modified oligothiophene crystals

YONG HU, JUN YIN, XUE-HAI JU\*

*Key Laboratory of Soft Chemistry and Functional Materials of MOE, School of Chemical Engineering, Nanjing University of Science and Technology, Nanjing 210094, P. R. China*

Density functional theory (DFT) was employed to calculate the property of some single-crystal organic semiconductors. The oligothiophene derivatives from **1** to **5** were studied from the aspects of frontier molecular orbital energy (HOMO, LUMO), bandgap ( $E_g$ ), ionization energy ( $IE$ ) and electron affinity ( $EA$ ), reorganization energy ( $\lambda$ ), hopping distance ( $r_i$ ) and overlap integral ( $H$ ) during the hole and electron transfer process. The charge mobility was calculated by Marcus theory and Einstein relation. As the number of thiophene conjugate ring increase, the energy level of LUMO, the bandgap and reorganization energy ( $\lambda$ ) have a trend of decrease. And the longer the main chain, the better the coplanarity. At the same time, the  $IE$  and  $EA$  have an opposite trend, the  $IE$  increasing while  $EA$  decreasing. These indicate that increasing the  $\pi$ -conjugate ring can make it easier of both electron and hole injection. The phene ring overlap and the interaction between adjacent molecules have a great influence on the charge transfer integral ( $H$ ) which is essential for large charge mobility value. These series of oligothiophene compounds turn their nature from  $p$ -type to  $n$ -type by introducing perfluoroarene rings to the parent molecule, and the electron mobility ( $\mu_-$ ) of compound **5** is  $0.19 \text{ cm}^2 \cdot \text{V}^{-1} \cdot \text{s}^{-1}$ , which is large enough to meet the requirement of a  $n$ -type organic semiconductor.

(Received April 15, 2015; accepted September 9, 2015)

*Keywords:* DFT; Charge mobility; Marcus theory; Organic semiconductor; Oligothiophene

## 1. Introduction

Organic semiconductor (OSC) is a kind of material which has a wide potential application. Since 1986, this field has attracted more and more attention and has made many achievements.<sup>1</sup> OSC has so many unique properties such as adaptability to low-temperature processing on flexible substrate, low cost, light weight, amenability to high-speed fabrication, and tunable electronic properties<sup>2-7</sup> compared to traditional inorganic materials. These features make them likely to replace the inorganic semiconductor materials which has been applied widespread<sup>8</sup> and become the major role in next generation electronic industry.<sup>9</sup> In recent years, great progress has been made in developing new OSC. A variety of new molecules with high charge mobility have been synthesized in thin films and single-crystal especially for  $p$ -type OSC<sup>10-12</sup> whose mobility is almost as large as amorphous silicon.<sup>13</sup> In contrast, the development of  $n$ -type OSC did not reach the same level of large mobility as  $p$ -type analogue.  $n$ -Type OSC with good atmosphere stability are still rare at the same time. It is obvious that the shortage of high-quality  $n$ -type OSC hindered its application such as

complementary integrated circuits, organic p-n junctions and bipolar transistors. So it is important to search for high performance ambient-stable  $n$ -type OSC.

Thiophene oligomer materials have been developed by Samulski<sup>14</sup> and have attracted much attention because of their special properties and potential application in many fields such as in organic light-emitting diodes (OLED) and in organic thin-film transistors. Some papers<sup>15-18</sup> reported that the connection of two aromatic rings of oligo phenylenes and thiophenes leads to diversity of molecular shapes and properties. A series of perfluoroarene modified oligothiophene compounds have been synthesized,<sup>19-22</sup> single-crystal structures have also been measured and parts of them were used in organic thin-film transistor device. Thus, this kind of molecules has promising application prospects and worthy of in-depth study. Theoretical study is another important method to explore these kinds of properties. In this work we presented a detailed theoretical study and a better understanding for the charge transfer properties of the title compounds. These oligothiophenes are 5,5'-diperfluorophenylthiophene (**1**), 5,5'-diperfluorophenyl-2,2'-dithiophene (**2**), 5,5''-

diperfluoro-phenyl-2,2':5',2''-terthiophene (3), 5,5''-diperfluoro phenyl-2,2':5',2''':5''', 2'''-quarterthiophene (4) and 5,5'-bis{1-[4-(thien-2-yl)perfluorophenyl]}-2,2'-dithiophene (5), Their reorganization energy ( $\lambda$ ), the energy level of the frontier molecular orbitals (HOMO, LUMO), the band gap ( $E_g$ ), the ionization energy ( $IE$ ) and electron affinity

( $EA$ ), the charge transfer integral between the dimer, and the charge mobility ( $\mu$ ) were calculated and analyzed to probe the inherent organic semiconductor properties of these series compounds on the basis of their single-crystal structures. Figure 1 showed the molecular structures and their unit cells of 1 to 5.

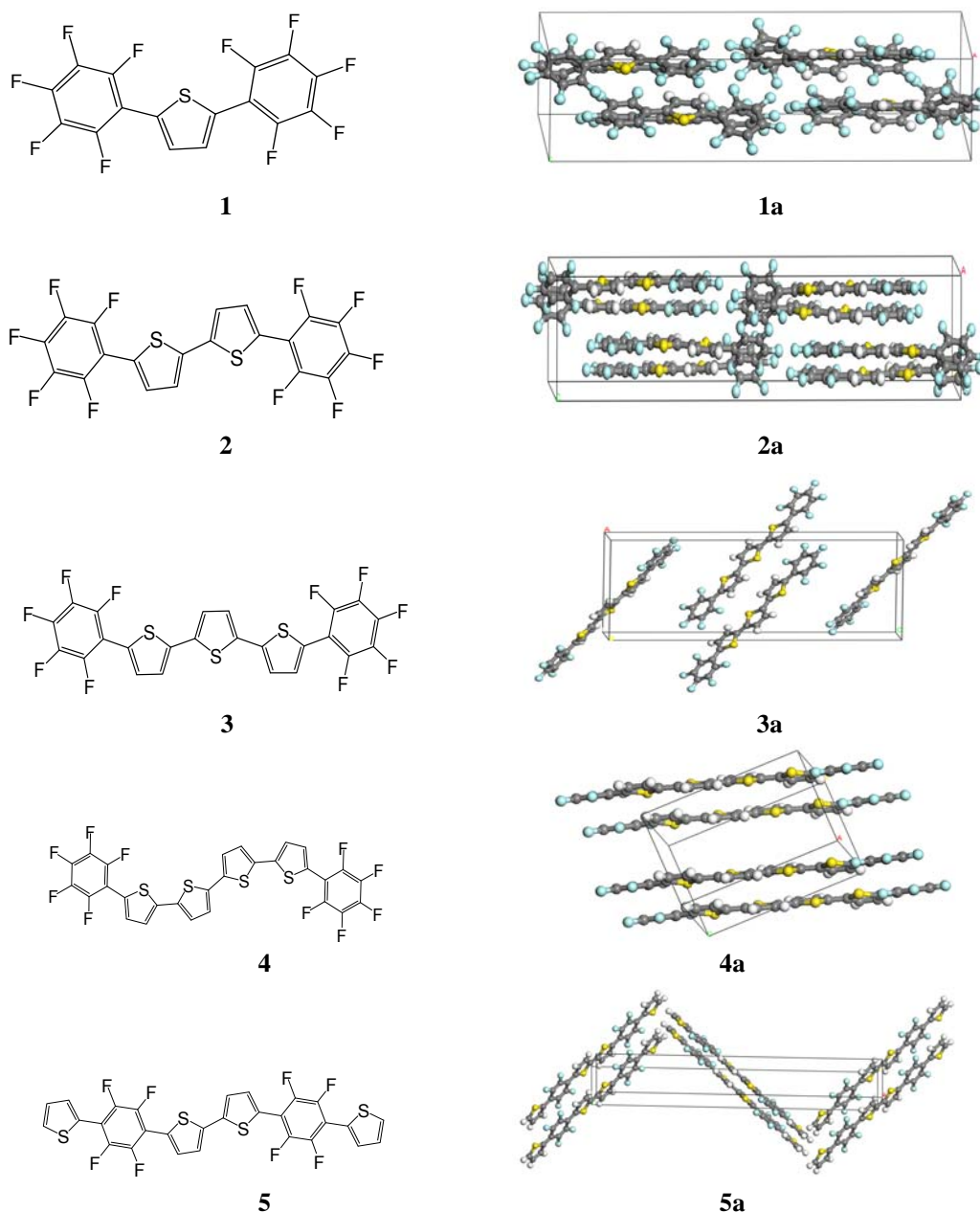


Fig.1 Molecular structures of oligothiophenes and their unit cells

## 2. Computational methods

We choose the incoherent hopping model but not the typical coherent band mode or other modes<sup>23</sup> to simulate the carrier motion in the solid state because coherent band

model is more suitable at low temperature and single crystal with highly ordered inorganic system while the hopping model<sup>25-28</sup> is much more suitable for the relatively weak coupling organic semiconductor system. In this mode, charge transfer is described as a self-exchange

electron transfer reaction between a neutral molecule and a neighboring radical cation (*p*-type) or radical anion (*n*-type). Charge mobility ( $\mu$ ) depends on both the reorganization energy ( $\lambda$ ) and the charge transfer integral ( $H$ ). We only focus on inner reorganization energy because we discussed about single-crystal systems without influence of solution or other external environment as many papers reported.<sup>5, 25-26</sup> Reorganization energy  $\lambda_+$  and  $\lambda_-$ , for hole and electron transfer respectively, can be calculated by the equation (1)

$$\lambda_{\pm} = (E_{\pm}^* - E_{\pm}) + (E^* - E) \quad (1)$$

where  $E$  respects the energy of neutral molecule in neutral geometry while  $E_{\pm}$  respects the energy of cation or anion molecule in cationic or anionic geometry. Then  $E^*$  and  $E_{\pm}^*$  are the energy of neutral molecules in cationic or anionic geometry and cation or anion molecule in neutral geometry, respectively. The rate constant for charge transfer ( $w$ ) is described by the follow equation (2) in classical Marcus theory:

$$w = \frac{H_{\text{eff}}^2}{\hbar} \left( \frac{\pi}{\lambda k_{\beta} T} \right)^{1/2} \exp\left(-\frac{\lambda}{4k_{\beta} T}\right) \quad (2)$$

The charge mobility can be evaluated by Einstein relation<sup>26</sup> for a given temperature:

$$\mu = eD(k_{\beta} T)^{-1} \quad (3)$$

where  $D = (2n)^{-1} \sum r_i^2 w_i p_i$ , and  $p_i = w_i / \sum w_j$ ,  $n$  is the dimensionality,  $r$  is the distance between the centers of mass of two adjacent molecules in the crystal,  $T$  is the temperature (in this work,  $T=298.15$  K) and  $k_{\beta}$  is the Boltzmann constant.  $H_{\text{eff}}$  is another important parameter besides  $\lambda$ . In this paper, the effective charge transfer integral is defined by following formula.

$$H_{\text{eff}} = \frac{H - \frac{1}{2}S \cdot (E_1 + E_2)}{1 - S^2} \quad (4)$$

where the  $E_1$  and  $E_2$  are the site energies of two monomers frontier molecular orbital while the  $S$  means the spatial overlap. The charge transfer integral is obtained by following equation.

$$H = \langle \psi_i | h_{ks} | \psi_j \rangle \quad (5)$$

the off-diagonal elements of the Kohn-Sham Hamiltonian matrix expressed as  $h_{ks} = S \cdot C \cdot E \cdot C^{-1}$  where the  $S$ ,  $C$  and  $E$  are intermolecular overlap matrix, molecular orbital coefficient and the molecular orbital energy, respectively. This method has been applied widely and shown its accuracy.<sup>27, 29, 30</sup> In this work, we chose density functional theory (DFT) method at the B3LYP/6-31G(d) level to optimize the molecules in neutral and ionic radical. While the HOMO and LUMO energy were obtained by the PBEPBE functional coupling with 6-31+G\* basis set. The B3LYP function was employed widely for calculating reorganization energy and proved to be consistent well with the experiment value. The charge transfer integral calculation was performed at PW91PW91/6-31G(d) level. All quantum chemical calculations were performed with Gaussian 09 program.<sup>31</sup>

### 3. Results and Discussion

#### 3.1. HOMO LUMO and the gap

The energy of frontier molecular orbital is an important concept for organic semiconductor. Figure 2 showed the energy of HOMO, LUMO and the  $E_g$  at the PBEPBE/6-31+G\* level for **1** to **5**. The LUMO energies are  $-3.17$  eV,  $-3.28$  eV and  $-3.31$  eV for **1**, **2** and **3**, respectively. **4** has same LUMO value with **3**, While the LUMO energy of **5** has the smaller negative value of  $-3.25$  eV. These negative LUMO energies are beneficial to the electron injection<sup>32</sup> and atmosphere stability<sup>13</sup>. At the same time, the HOMO energies have an opposite trend. From **1** to **4**, the HOMO energies increase obviously, while that of **5** has a small decrease in comparison with **4**. This increase trend also occurs in other oligomers.<sup>34</sup> Combining these two opposite trends, it is easy to understand the decrease trend of HOMO-LUMO gaps that also exists in other oligomers.<sup>35</sup> Parts of experimental gaps were also showed in the brackets. Although the calculated gaps are not consistent with the experimental values as some papers reported,<sup>36</sup> variations of the gaps from **1** to **5** are similar. Some reasons may cause these differences such as the inherent defects of the DFT theory, the defective devices or film in the experiment or the experimental error.

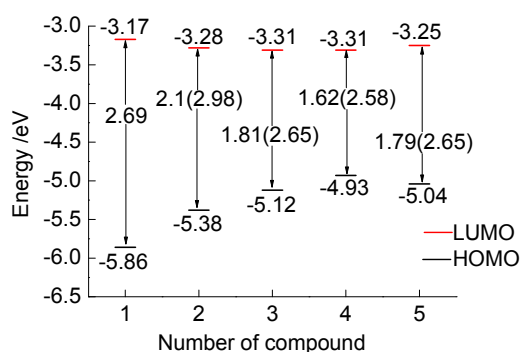


Fig. 2. The energies of LUMO/HOMO and their gap, data in brackets is experimental value

In order to explain the HOMO/LUMO trends, the frontier molecular orbital topologies (both HOMO and LUMO) were displayed in Figure 3. It can be seen that the HOMO is distributed over the whole molecule of **1**, the HOMO of **2** has a less portion of distribution at the end aromatic rings, and for **3** and **4**, these trends look more and more obvious as compared with **1**. These mean that the

HOMO of the molecules depend more and more on the wave function of inner thiophene rings, while the contribution of the end perfluorinated phenyl rings to the HOMO becomes less and less from **1** to **4**. The LUMO distribution of **1** to **4** also concentrated on the inner thiophene rings, but the trend is not as obvious as the HOMO distribution. At the same time, as the perfluorinated phenyl rings moved from the end to the inner, **5** shows a little different. Both HOMO and LUMO distribution of **5** on the fluorinated phenyl rings have a little increase relative to **4** and reverse the trend of decrease gradually. It should be mentioned that the coplanarity of these molecular as shown in Figure 4 are different. The coplanarity of **3**, **4** and **5** are better than **1** and **2**. The lateral fluorinated phenyl ring can make HOMO and LUMO distribution concentrate to the conjugated oligothiophene rings if the coplanarity of the molecule is well enough. Moving the fluorinated phenyl rings from the end to the inner has obvious effects on both HOMO/LUMO topologies and their energies for **1** to **4** as shown in Fig. 3 and Fig. 2.

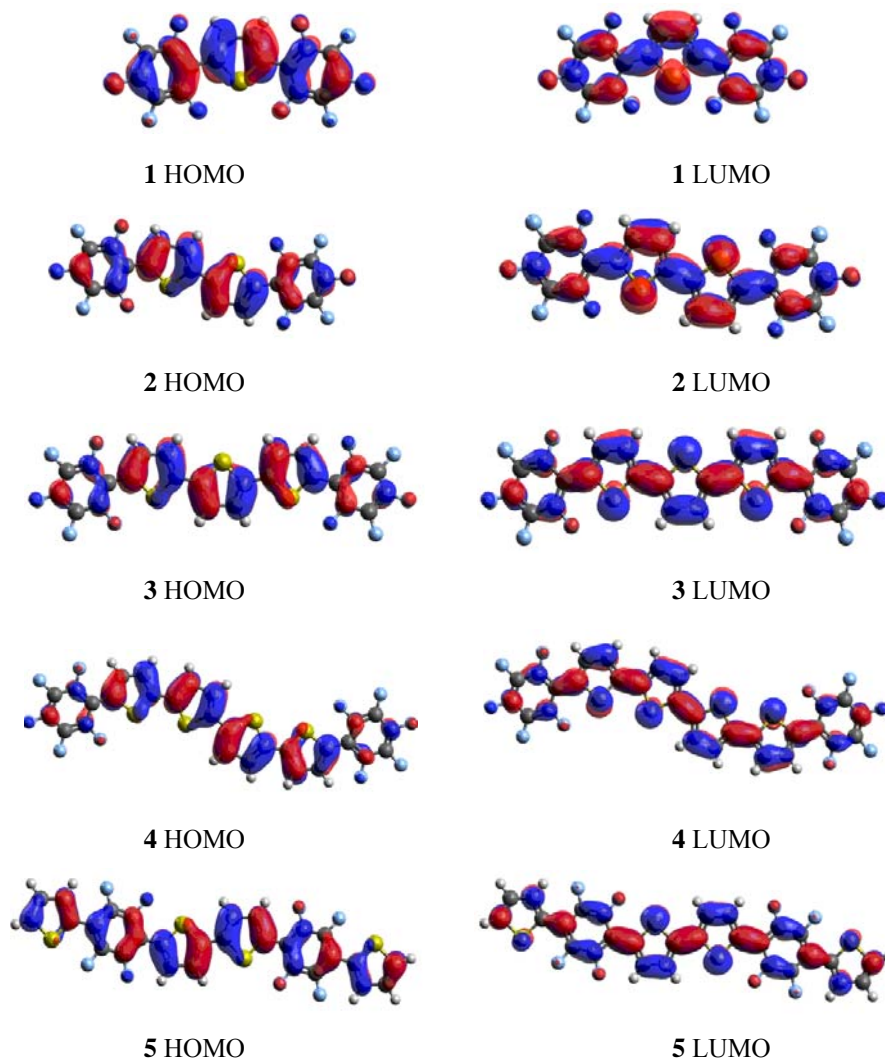


Fig. 3. Topologies of frontier molecular orbital (HOMO and LUMO) for **1** to **5**

### 3.2. EA, IE and reorganization energy

Besides the energy of frontier molecular orbitals (HOMOs/LUMOs), both the ionization energy ( $IE$ ) and electron affinity ( $EA$ ) offer more information about the charge transfer. Table 1 listed the adiabatic ionization energy ( $IE_a$ ), vertical ionization energy ( $IE_v$ ), the adiabatic electron affinity ( $EA_a$ ) and vertical electron affinity ( $EA_v$ ), which were calculated by DFT at B3LYP/6-31+G\* level. It is well-known that the injection barrier to some extent decides the type of charge injected into the organic semiconductor from source materials. Electron affinity and ionization energy reflect the barrier of electron and hole injection, respectively. A well-performance  $n$ -type OSC needs enough high electron affinity to allow electron inject into LUMO, but a high-quality  $p$ -type OSC have to make its ionization energy as low as possible on the contrary. According to Table 1, **4** and **5** have the largest  $EA$  and the relatively smallest  $IE$ , and it seems that both of them have a potential to be either  $n$ -type or  $p$ -type OSC in view of  $EA$  and  $IE$ . And it is obvious that the electron affinity has an increasing trend from **1** to **5**, while the ionization energy tends to decrease at the same time. This is consistent with HOMO and LUMO levels. Both the HOMO and LUMO tend to distribute over the middle thiophene rings and the conjugate planar becomes larger and smoother, which makes electron and hole injection more easier<sup>32</sup>.

Reorganization energy is an important parameter which has a great influence to the charge mobility according to equation (2). When an electron injects into or removes away from a molecule, the molecule has to change its geometric structure and release or absorb some energy during these processes. In order to get a large  $\mu$ , the reorganization energy should be as small as possible. Table 1 presented both hole and electron reorganization energy of **1** to **5**. It is obvious that **1** has the largest electron and hole reorganization energy which is in consistent with its smallest electron affinity level and largest ionization energy. Therefore, it is more difficult for **1** to inject or to remove electron than others, because it has the most uneven conjugated plane that is not suit for internal site energy relaxation. As the number of thiophene rings increase to 2, the reorganization level (both electron and hole) have an obvious decrease from 0.420 eV to 0.351 eV for  $\lambda_+$  (from 0.367 eV to 0.310 eV for  $\lambda_-$ ). Both  $\lambda_+$  and  $\lambda_-$  have a decrease trend from **1** to **5** except for **4**.

The abnormal trend of **4** is caused by its cis-arrangement of the adjacent thiophene rings in **4** molecule. These two cis-thiophene pairs lead to the increasing of inner stereo-hindrance and are not conducive to the internal site energy relaxation. Compound **5** has the smallest  $\lambda$  that is in favor of internal site energy relaxation. This is in consistent with the large conjugated plane for **5**. From the viewpoint of  $\lambda$ , **5** is a high-performance OSC with its small  $\lambda_-$  and  $\lambda_+$ , which may be own to its excellent coplanarity, and another possible reason may be that the hexatomic rings in middle chain have a smaller ring tension than five-membered thiophene ring and can decrease the internal stress in some extent. The increasing numbers of conjugate rings contribute a lot to the reorganization energy decreasing which is also mentioned in some paper<sup>34,26</sup>.

Table 1 Adiabatic energy ( $IE_a$ ), vertical ionization energy ( $IE_v$ ), adiabatic energy ( $EA_a$ ), vertical electron affinity ( $EA_v$ ), hole reorganization energy ( $\lambda_+$ ) and electron reorganization energy ( $\lambda_-$ ) for all compounds \*

| Compound | $EA_a$ | $EA_v$ | $IE_a$ | $IE_v$ | $\lambda_+$ | $\lambda_-$ |
|----------|--------|--------|--------|--------|-------------|-------------|
| <b>1</b> | 0.722  | 0.943  | 7.59   | 7.39   | 0.367       | 0.420       |
| <b>2</b> | 1.06   | 1.24   | 6.94   | 6.78   | 0.310       | 0.351       |
| <b>3</b> | 1.25   | 1.43   | 6.56   | 6.40   | 0.298       | 0.328       |
| <b>4</b> | 1.36   | 1.55   | 6.36   | 6.11   | 0.316       | 0.341       |
| <b>5</b> | 1.35   | 1.47   | 6.38   | 6.26   | 0.235       | 0.242       |

\* All data are in eV.

### 3.3. Intermolecular charge transfer integral and Charge mobility

We selected all possible hopping paths from the single-crystal structures and simulated all dimers by Marcus hopping theory. Besides reorganization energy, the effective intermolecular charge transfer integral ( $H_{eff}$ ) is another important parameter that has great influence to charge mobility ( $\mu$ ). The larger the  $H_{eff}$ , the larger the  $\mu$  will be. Because of different molecular structure and molecular symmetry, the molecular packing and the number of dimer are not exactly the same. These factors result in a large difference of the  $H_{eff}$ . Table 2 offers some possible hopping pathway and its corresponding effective hole transfer integral ( $H_h$ ) and effective electron transfer integral ( $H_e$ ).

Table 2 Electronic coupling for 1 to 5 at PW91PW91/6-31G(d) level \*

| Compound | n | $H_e$ (meV) |           |           | $H_h$ (meV) |           |           |
|----------|---|-------------|-----------|-----------|-------------|-----------|-----------|
| <b>1</b> | 6 | (1) 80.01   | (2) -0.50 | (3) 6.90  | (1) -135.5  | (2) 1.90  | (3) -1.80 |
|          |   | (4) -0.50   | (5) 6.90  | (6) 24.5  | (4) 1.90    | (5) -1.80 | (6) -40.0 |
| <b>2</b> | 9 | (1) 5.20    | (2) 5.20  | (3) 5.20  | (1) 71.21   | (2) 0.30  | (3) 0.30  |
|          |   | (4) -6.40   | (5) -5.20 | (6) -18.5 | (4) 0.30    | (5) 1.30  | (6) -13.7 |
|          |   | (7) 1.90    | (8) -2.10 | (9) 1.90  | (7) 2.00    | (8) 0.50  | (9) 2.00  |
| <b>3</b> | 5 | (1) 19.2    | (2) 27.40 | (3) 4.10  | (1) -138.5  | (2) -1.20 | (3) 0.90  |
|          |   | (4) -0.40   | (5) -0.40 |           | (4) 0.60    | (5) 0.60  |           |
| <b>4</b> | 3 | (1) 10.2    | (2) -12.1 | (3) 31.70 | (1) -5.90   | (2) 52.7  | (3) -8.40 |
| <b>5</b> | 7 | (1) 59.7    | (2) 2.10  | (3) -0.30 | (1) 28.9    | (2) -2.40 | (3) -0.30 |
|          |   | (4) -4.50   | (5) 0.80  | (6) -4.50 | (4) 5.60    | (5) 0.20  | (6) 5.60  |
|          |   | (7) 0.80    |           |           | (7) 0.20    |           |           |

\* n is the number of hopping pathways. The digitals in brackets denote the different pathways.

From **1** to **5**, all the largest  $H_h$  values derive from path 1 which are always much larger than the corresponding  $H_h$  values except for **4**. The largest  $H_h$  of **4** comes from path 2. The  $H_h$  value in **1** from path 6 is 40 meV, far less than 135.5 meV, the largest  $H_h$ . For **3**, the largest  $H_h$  of path 1 is almost 140 times to the second largest  $H_h$  from path 2. Some pathways hardly contribute to  $H_h$ . In one word, the largest  $H_h$  always makes the most contribution while the  $H_h$  from some other pathways can be ignored as many publications pointed out.<sup>37</sup> And there is an obvious decrease trend from **1** to **5** for largest  $H_h$  value. There are some differences in  $H_e$ . First, the largest  $H_e$  does not always come from path 1, such as **2**, **3** and **4**, their largest contributions derive from paths 6, 2 and 3 respectively, and the difference between the largest  $H_e$  and the second one are not as large as  $H_h$ . The second largest  $H_e$  of **3** is 19.2 meV and roughly close to the largest  $H_e$  27.4 meV, even though the spatial overlap of though path 2 which contribute the largest  $H_e$  is much smaller than path 1 (Fig. 4). These mean that the main hopping pathway for hole and electron are not always exactly same, and there must have other factors which can also contribute effective electron transfer. It can be found that the largest  $H_h$  value is larger than the largest  $H_e$  for **1** to **4**, while there is a reverse order for **5**. These indicate that their hole mobility

( $\mu_+$ ) will likely to be larger than electron mobility ( $\mu_-$ ) except for **5** from the charge transfer integral aspect if take the index of  $H_{eff}$  in equation 2 into account.

Fig. 4 showed some hopping routes. It is obvious that path 1 has the best conjugate overlap which is essential for large  $H_{eff}$  value between adjacent molecules. It can be seen in Fig. 4, two perfluorinated phene rings in route 6 of **2** have a well overlap and the vertical distance of the face-to-face phene rings is 3.3 Å. The overlap of perfluorinated phene rings is greatly beneficial to the electron hopping. Both paths 3 and 2 of **4** contribute a larger  $H_e$  than path 1. These should be mainly due to the interaction of F atom and thiophene ring, the nearest distance of them are 2.58 Å which is suitable to produce a relative strong effect. The nearest distance of face-to-face aromatic rings in path 1 is 3.36 Å, larger than those of paths 2 and 3. In **3**, path 2 also has a larger  $H_e$  value than path 1 due to the fact that the shortest hopping distance of path 2 is 2.65 Å, shorter than 3.22 Å of path 1. It means that both effective overlap of aromatic conjugate ring and hopping distance have a great influence to the  $H_{eff}$  value. And the weak interaction between the two monomers can also make an additional contribution to electron transfer.<sup>11, 16</sup>

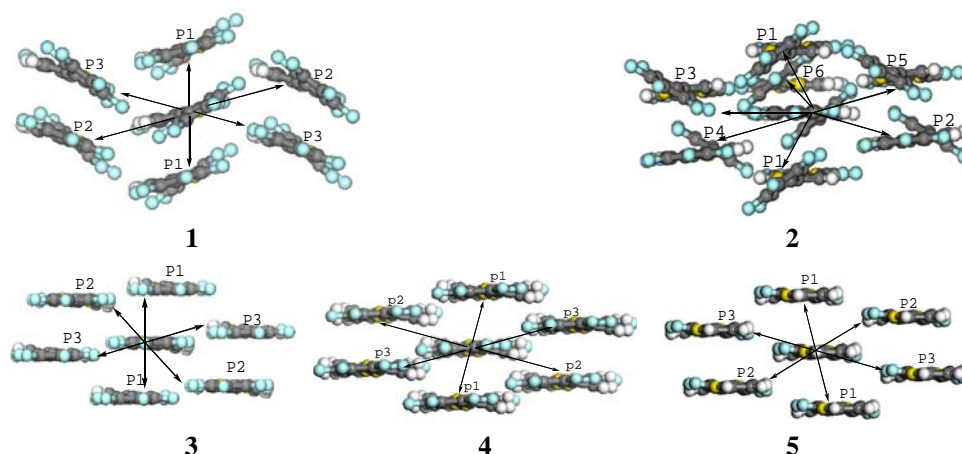


Fig.4 Schemes of main electron-hopping routes for 1 to 5

The charge mobility values of both  $\mu_-$  and  $\mu_+$  calculated by Marcus equation and Einstein relation were listed in Table 3. The  $\mu_-$  of these series compounds are smaller than  $\mu_+$  except for **5**.  $\mu_+$  of **1**, **2**, **3** and **4** are  $0.28 \text{ cm}^2 \cdot \text{s}^{-1} \cdot \text{V}^{-1}$ ,  $0.21 \text{ cm}^2 \cdot \text{s}^{-1} \cdot \text{V}^{-1}$ ,  $0.72 \text{ cm}^2 \cdot \text{s}^{-1} \cdot \text{V}^{-1}$  and  $0.39 \text{ cm}^2 \cdot \text{s}^{-1} \cdot \text{V}^{-1}$ , respectively. These values are all larger than their corresponding  $\mu_-$  values, indicating that these compounds good *p*-type OSC rather than *n*-type. From the perspective of  $H_{eff}$ , the largest  $H_e$  from special pathway which contributes the largest  $H_h$  is smaller obviously than its respective  $H_h$  for **1**, **2**, **3** and **4**. The largest  $H_h$  of **3** is 138.5 meV, which is bigger than any others  $H_{eff}$  value, leading to its largest  $\mu_+$ ,  $0.72 \text{ cm}^2 \cdot \text{s}^{-1} \cdot \text{V}^{-1}$ . The largest  $H_h$  of **1** is 135.45 meV, very similar to **3**. However, there is a large difference between the  $\mu_+$  values of **1** and **3**, due to the difference of their  $\lambda_+$  values. Although a large  $H_{eff}$  is essential for high performance OSC, other factors such as and hopping distance ( $r_i$ ) of the main paths and the  $\lambda$  are also important in the charge mobility. The  $\mu_-$  of **5** is  $0.19 \text{ cm}^2 \cdot \text{s}^{-1} \cdot \text{V}^{-1}$ . It should be mentioned that the  $H_e$  value of **5** is second largest  $H_e$  in Table 2, while the  $\mu_-$  of **5** is the largest. This is caused by the difference of  $\lambda$ , as mentioned above. **5** is the only compound whose  $\mu_-$  is larger than its  $\mu_+$ , since its  $H_e$  is larger than  $H_h$ . **5** could be an *n*-type OSC.

Table 3 Hole and electron mobility for compounds 1 to 5

| Charge mobility   | <b>1</b> | <b>2</b> | <b>3</b> | <b>4</b> | <b>5</b> |
|---|----------|----------|----------|----------|----------|
| $\mu_- (\text{cm}^2 \cdot \text{s}^{-1} \cdot \text{V}^{-1})$ | 0.054    | 0.026    | 0.018    | 0.091    | 0.19     |
| $\mu_+ (\text{cm}^2 \cdot \text{s}^{-1} \cdot \text{V}^{-1})$ | 0.28     | 0.21     | 0.72     | 0.39     | 0.047    |

#### 4. Conclusion

A series of perfluoroarene modified oligothiophene compounds were investigated by the DFT calculations. We

analyzed the charge mobility by probing the influence of frontier molecular orbital energy, bandgap, ionization energy ( $IE$ ) and electron affinities ( $EA$ ), reorganization energy ( $\lambda$ ) hopping distance ( $r_i$ ) and overlap integral ( $H$ ). The introduction of the end perfluorinated phene rings can reduce the barrier of electron injection while increase the barrier of hole injection. When the perfluorinated phene rings were transferred from the end to the middle, these effects will decrease in some degree. Reorganization energy decreases as the number of thiophene conjugate rings increasing. The packing pattern of the dimers has a great influence to the effective overlap integral ( $H_{eff}$ ) which is essential for high charge mobility, while the difference of molecular structure and planarity lead to a great different of molecule packing in unit cell. The largest  $H$  focuses on a few effective hopping pathways with perfect  $\pi$ -conjugate overlap or some internal molecular interaction between the two monomers, while other dimers hardly make contributions to the final charge mobility. **3** has many favorable factors which make its promising application prospect as a *p*-type OSC, while **5** looks like to be an *n*-type OSC. The inherent natures make the oligothiophenes to be *p*-type OSC, but the introduction of the perfluorinated phene rings can make a great change to their properties and can turn them to the *n*-type OSC. A further study to understand the relation between some other factors such as the number of phene ring, the number of F atom, the different others location of the substituent group and others electron-withdrawing group and the OSC properties will be a meaningful and well-prospective work.

#### Acknowledgements

The authors thank the National Science Foundation of China (No. 21372116) for supporting this work.

## References

- [1] A. Tsumura, H. Koezuka, Ando, T.; *Appl. Phys. Lett.*, **49**, 1210 (1986).
- [2] L. Tan, L. Zhang, X. Jiang, X. D. Yang, L. J. Wang, Z. H. Wang, L. Q. Li, W. P. Hu, Z. G. Shuai, L. Li, D. B. Zhu, *Adv. Funct. Mater.*, **19**, 272 (2009).
- [3] M. Kitamura, T. Imada, Y. Arakawa, *Appl. Phys. Lett.*, **83**, 3410 (2003).
- [4] C. R. Newman, C. D. Frisbie, D. A. Da Silva Filho, J. L. Brédas, P. C. Ewbank, K. R. Mann, *Chem. Mater.*, **16**, 4436 (2004).
- [5] L. J. Wang, G. J. Nan, X. D. Yang, Q. Peng, Q. k. Li, Z. G. Shuai, *Chem. Soc. Rev.*, **39**, 423 (2010).
- [6] M. Y. Chikamatsu, A. Itakura, Y. J. Yoshida, R. K. Azumi, K. Yase, *Chem. Mater.*, **20**, 7365 (2008).
- [7] Q. J. Sun, G. F.; Dong, H. Y. Zheng, H. Y. Zhao, J. Qiao, L. Duan, L. D. Wang, F. S. Zhang, Y. Qiu *Acta Phys. -Chim. Sin.*, **27**, 1893 (2011).
- [8] J. Teteris, M. Reinfelde, *J. Optoelectron. Adv. Mater.*, **5**, 1355 (2003).
- [9] C. D. Dimitrakopoulos, P. R. L. Malenfant, *Adv. Mater.*, **14**, 99 (2002).
- [10] S. W. Yun, J. H. Kim, S. Shin, H. Yang, B. K. An, L. Yang, S. Y. Park, *Adv. Mater.*, **24**, 911 (2012).
- [11] J. K. Lee, B. S. Jeong, J. Kim, C. Kim, J. Ko. *Photoch. Photobio. A.*, **251**, 25 (2013).
- [12] T. M. F. Duarte, K. Müllen, *Chem. Rev.*, **111**, 7260 (2011).
- [13] H. Klauk, M. Halik, U. Zschieschang, G. Schmid, W. Radlik, *J. Appl. Phys.*, **92**, 5259 (2002).
- [14] S. Hotta, S. A. Lee, *Synth. Met.*, **101**, 551 (1999).
- [15] M. H. Yoon, A. Facchetti, C. E. Stern, T. J. Marks, *J. Am. Chem. Soc.*, **128**, 5792 (2006).
- [16] S. Mohapatra, B. T. Holmes, C. R. Newman, C. F. Prendergast, C. D. Frisbie, M. D. Ward, *Adv. Funct. Mater.*, **14**, 605 (2004).
- [17] V. C. Ackermann, J. Ackermann, J. Ackermann, H. Brisset, K. Kawamura, N. Yoshimoto, P. Raynal, A. El Kassmi, F. Fages, *J. Am. Chem. Soc.*, **127**, 16346 (2005).
- [18] S. Hotta, T. J. Katagiri, *Heterocycl. Chem.*, **40**, 845 (2003).
- [19] A. Facchetti, J. Letizia, M. H. Yoon, M. Musherush, H. E. Katz, T. Marks, *J. Chem. Mater.*, **16**, 4715 (2004).
- [20] H. E. Katz, T. Siegrist, M. Lefenfeld, P. Gopalan, M. Musherush, B. Ocko, O. Gang, N. Jisrawl, *J. Phys. Chem. B*, **108**, 8567 (2004).
- [21] M. Musherush, A. Facchetti, M. Lefenfeld, H. E. Katz, T. J. Marks, *J. Am. Chem. Soc.*, **125**, 9414 (2003).
- [22] N. Cho, K. Song, J. K. Lee, J. Ko, *Chem. Eur. J.*, **18**, 11433 (2012).
- [23] G. J. Nan, R. H. Zheng, Q. Shi, Z. G. Shuai, *Acta Phys. -Chim. Sin.*, **26**, 1755 (2010).
- [24] H. Geng, Q. Peng, L. J. Wang, H. J. Li, Y. Liao, Z. Y. Ma, Z. G. Shuai, *Adv. Mater.*, **24**, 3568 (2012).
- [25] M. X. Zhang, G. J. Zhao, *Chem. Sus. Chem.*, **5**, 879 (2012).
- [26] S. Chai, S. H. Wen, J. D. Huang, K. L. Han, *J. Comput. Chem.*, **32**, 3218 (2011).
- [27] C. B. Zhao, W. L. Wang, S. W. Yin, Y. Ma, *New J. Chem.*, **37**, 2925 (2013).
- [28] G. Wang, *J. Synth. Met.*, **160**, 599 (2010).
- [29] M. M. Mikolajczyk, R. Zaleśny, Z. Czyżnikowska, P. Toman, J. Leszczynski, Bartkowiak, W. J. *Mol. Model.*, **17**, 2143 (2011).
- [30] S. H. Wen, A. Li, J. L. Song, W. Q. Deng, K. L. Han, W. A. Goddard, *J. Phys. Chem. B*, **113**, 8813 (2009).
- [31] M. J. Frisch, G. W. Trucks, H. B. Schlegel, G. E. Scuseria, M. A. Robb, J. R. Cheeseman, G. Scalmani, V. Barone, B. Mennucci, G. A. Petersson, H. Nakatsuji, M. Caricato, X. Li, H. P. Hratchian, A. F. Izmaylov, J.; Bloino, G.; Zheng, J. L. Sonnenberg, M. Hada, M. Ehara, K. Toyota, R. Fukuda, J. Hasegawa, M. Ishida, T. Nakajima, Y. Honda, O. Kitao, H. Nakai, T. Vreven, J. A. Montgomery, Jr.; J. E. Peralta, F. Ogliaro, M. Bearpark, J. J. Heyd, E. Brothers, K. N. Kudin, V. N. Staroverov, R. Kobayashi, J. Normand, K. Raghavachari, A. Rendell, J. C. Burant, S. S. Iyengar, J. Tomasi, M. Cossi, N. Rega, J. M. Millam, M. Klene, J. E. Knox, J. B. Cross, V. Bakken, C. Adamo, J. Jaramillo, R. Gomperts, R. E. Stratmann, O. Yazyev, A. J. Austin, R. Cammi, C. Pomelli, J. W. Ochterski, R. L. Martin, K. Morokuma, V. G. Zakrzewski, G. A. P.; Voth, J. J. Salvador, Dannenberg, Dapprich, S.; Daniels, A. D.; Farkas, Ö.; Foresman, J. B.; Ortiz, J. V.; Cioslowski, J.; Fox, D. J. *Gaussian 09*, Revision C. 03; Gaussian Inc.: Wallingford, CT, 2010.
- [32] S. W. Yun, J. H. Kim, S. Shin, H. Yang, B-K. An, L. Yang, S. Y. Park, *Adv. Mater.*, **24**, 911 (2012).
- [33] I. Osaka, S. J. Shinamura, T. Abea, K. Takimiya, *J. Mater. Chem. C*, **1**, 1297 (2013).
- [34] N. A. Sánchez-Bojorge, L. M. Rodríguez-Valdez, N. J. Flores-Holguín, *Mol. Model.*, **19**, 3537 (2013).
- [35] P. Sonar, S. P. Singh, T. T. Lin, A. Dodabalapur, *Aust. J. Chem.*, **66**, 370 (2013).
- [36] A. Zhong, Y. Z. Bian, Y. X. Zhang, *J. Phys. Chem. C*, **114**, 3248 (2010).
- [37] C. B.; Zhao, Y. L.; Guo, L.; Guan, H.; Ge, S. W.; Yin, W. L. Wang, *Synth. Met.*, **188**, 146 (2014).

\* Corresponding author: xhju@njust.edu.cn